Spacer-Length-Dependent Association in Polymers with Multiple-Hydrogen-Bonded End Groups

Tom F. A. De Greef,[1] Matthew J. Kade,[2] Kathleen E. Feldman,[4] Edward J. Kramer,[3,4] Craig J. Hawker,[2] E. W. Meijer[1]

[1]Institute for Complex Molecular Systems, Laboratory of Macromolecular and Organic Chemistry, Eindhoven University of Technology, P.O. Box 513, 5600 MB, Eindhoven, The Netherlands
[2]Department of Chemistry and Biochemistry, Materials Research Laboratory, University of California, Santa Barbara, California 93106
[3]Department of Chemical Engineering, Materials Research Laboratory, University of California, Santa Barbara, California 93106
[4]Department of Materials, Materials Research Laboratory, University of California, Santa Barbara, California 93106

Correspondence to: C. J. Hawker (E-mail: hawker@chem.ucsb.edu) or E. W. Meijer (E-mail: e.w.meijer@tue.nl)

Received 2 May 2011; accepted 29 June 2011; published online 26 July 2011
DOI: 10.1002/pola.24868

ABSTRACT: Herein, we investigate the influence of spacer length on the homoassociation and heteroassociation of end-functionalized hydrogen-bonding polymers based on poly(*n*-butyl acrylate). Two monofunctional ureido-pyrimidinone (UPy) end-functionalized polymers were prepared by atom transfer radical polymerization using self-complementary UPy-functional initiators that differ in the spacer length between the multiple-hydrogen-bonding group and the chain initiation site. The self-complementary binding strength (K_{dim}) of these end-functionalized polymers was shown to depend critically on the spacer length as evident from ^{1}H NMR and diffusion-ordered spectroscopy. In addition, the heteroassociation strength of the end-functionalized UPy polymers with end-functionalized polymers containing the complementary 2,7-diamido-1,8-naphthyridine (NaPy) hydrogen-bond motif is also affected when the aliphatic spacer length is too short. © 2011 Wiley Periodicals, Inc. J Polym Sci Part A: Polym Chem 49: 4253–4260, 2011

KEYWORDS: atom transfer radical polymerization (ATRP); diffusion-ordered spectroscopy; hydrogen bonding; supramolecular diblock copolymers

INTRODUCTION The combination of supramolecular chemistry and the controlled phase separation of diblock copolymers can result in a wealth of nanoscale morphologies with applications ranging from semiconductor integrated circuit design to the development of subnanometer porous films for separation processes.[1–4] Theoretical work has shown that the domain size and morphology of the phase-separated structures critically depend on the strength of the interpolymer noncovalent interactions.[5–10] To achieve these attractive enthalpic interpolymer interactions, end-functionalized homopolymers have been prepared with functional groups capable of noncovalent assembly such as hydrogen bonding,[11–20] ionic,[21] transition-metal,[22,23] host–guest,[24–26] and fluorophilic[27] interactions. Typically, these functional groups are attached to a homopolymer via a short, aliphatic spacer. Recent reports, however, have shown that the association strength of noncovalent assemblies can be decreased by competitive noncovalent interactions with functional groups present in the side-chains. For example, we have recently shown that the ureido-pyrimidinone (UPy) dimerization constant (K_{dim}) decreases by a factor of 1000 in chloroform when the UPy group is attached to a triethylene glycol (triEG) chain via a short C_2 spacer.[28,29] When the spacer length is increased from C_2 to C_6, no reduction in K_{dim} is observed compared with a UPy without an EG chain, suggesting that the reduction in K_{dim} is associated with competing intramolecular hydrogen bonding between the EG chain and the hydrogen-bond donors of the UPy group. In addition, Gibson and coworkers reported a ninefold decrease in association constant between polystyrene and poly(methyl methacrylate) (PMMA) functionalized "paraquats" and unfunctionalized crown-ethers.[26] The decrease in association constant was attributed to competing intramolecular interactions between the ester moieties of PMMA and the aromatic protons of the paraquat unit. Given the crucial role of the interpolymer noncovalent binding strength in determining the nanoscale morphology of supramolecular diblock copolymers, it becomes evident that great care should be exerted in the precise arrangement of the associating end groups with respect to the homopolymer.

Additional Supporting Information may be found in the online version of this article.

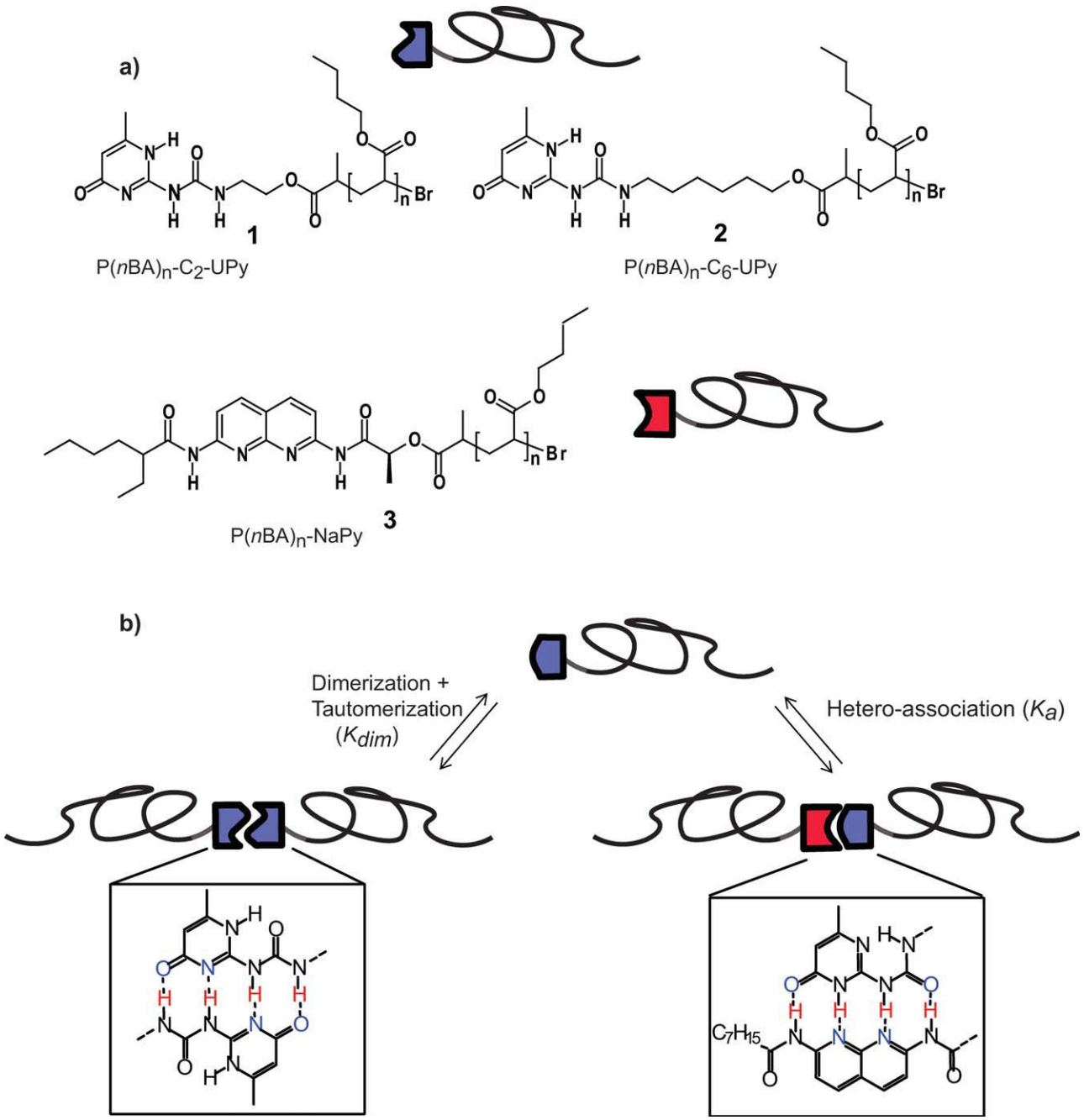

FIGURE 1 (a) Structures of multiple-hydrogen-bond end-functionalized P(nBA) polymers **1–3** and (b) their mode of supramolecular association.

Herein, we report a thermodynamic investigation of the quadruple hydrogen-bond strength of two UPy end-capped poly(*n*-butyl acrylate) (P*n*BA) polymers (further abbreviated as P(*n*BA)$_n$-C$_x$-UPy), which differ in the number of carbon atoms (x) of the aliphatic spacer separating the UPy group from the P*n*BA backbone. In addition, heteroassociation[30,31] of the UPy end-functionalized P*n*BA polymers with a 2,7-diamido-1,8-naphthyridine (NaPy) end-functionalized P*n*BA polymer was quantified by UV–Vis titrations to investigate whether the heteroassociation strength depends on the length of the aliphatic spacer of the UPy end-functionalized polymers.

RESULTS AND DISCUSSION

The structures of the investigated polymers **1–3** and their mechanism of association are displayed in Figure 1. All end-functionalized P*n*BA polymers were prepared from multiple-hydrogen-bonded functional initiators using an established atom transfer radical polymerization (ATRP) procedure.[12]

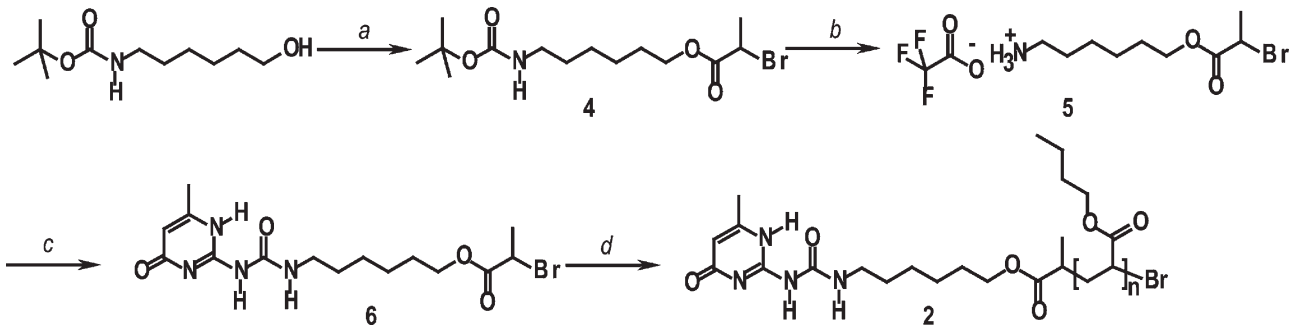

SCHEME 1 Synthetic route toward P(nBA)$_n$-C$_6$-UPy **2**: (a) 2-bromopropionyl bromide, pyridine, dichloromethane, 12 h, 0 °C then RT, 64%; (b) trifluoroacetic acid, dichloromethane, 14 h, 0 °C then RT, 93%; (c) 2-(1-imidazolylcarbonylamino)-6-methyl-4-[1H]-pyrimidinone, triethylamine, chloroform, 12 h, 50 °C, 50%; (d) *n*-butyl-acrylate (nBA), PMDETA, CuBr, 3 h, 70 °C.

The resulting molecular weight distributions of P*n*BA polymer **1**–**3** were monomodal and polydispersities were typically in the range of 1.1–1.2. P(nBA)$_n$-C$_2$-UPy **1**, in which a C$_2$ spacer connects the hydrogen-bonding end group to poly(*n*-butyl acrylate) was synthesized as previously described.[12] Size-exclusion chromatography (SEC; calibrated with linear polystyrene standards) using tetrahydrofuran as an eluent revealed that the number average molecular weight (M_n) of P(nBA)$_n$-C$_2$-UPy **1** is 9.8 kDa (Supporting Information, Fig. S1, polydispersity index (PDI) = 1.1). P(nBA)$_n$-C$_6$-UPy **2**, in which a C$_6$ spacer connects the hydrogen-bonding end group to the poly(*n*-butyl acrylate), was synthesized from *n*-butyl acrylate (*n*BA) and UPy ATRP initiator **6** at 70 °C using the CuBr/PMDETA system as a catalyst (Scheme 1).[32] The number average molecular weight of **2** was determined to be 8.9 kDa using SEC (Supporting Information, Fig. S2, PDI = 1.1, tetrahydrofuran as an eluent). Finally, P(nBA)$_n$-NaPy **3** (Supporting Information, Fig. S3, M_n = 18.5 kDa, PDI = 1.15) was synthesized as previously described.[12] The molecular weights and polydispersities of the end-functionalized polymers **1**–**3** are summarized in Table 1.

The ^{1}H NMR spectra of P(nBA)$_n$-C$_2$-UPy **1** and P(nBA)$_n$-C$_6$-UPy **2** in dry $CDCl_3$ at a concentration of 10 mM clearly show three sharp resonances in the downfield region (>9 ppm) of the spectrum indicative of extensive dimerization via quadruple-hydrogen bonding (Supporting Information, Figs. S4 and S5). Furthermore, the position of the alkylidene proton of the pyrimidinone ring for both UPy end-functionalized polymers at this concentration provides additional evidence for the formation of quadruple hydrogen-bonded dimers.[28,29]

TABLE 1 Molecular Weight Characterization of End-Functionalized P*n*BA Polymers **1–3** as Determined by SEC in THF

Polymer	M_n (kDa)	PDI	Spacer Length	Chain End
1	9.8	1.1	C$_2$	UPy
2	8.9	1.1	C$_6$	UPy
3	18.5	1.15	–	NaPy

To quantify the dimerization constant (K_{dim}) of the two UPy end-functionalized polymers in $CDCl_3$, ^{1}H NMR dilution experiments were performed on P*n*BA polymers **1** and **2**, which differ in the length of the aliphatic spacer connecting the multiple-hydrogen-bonded end group to the polymer.

Figure 2 displays the partial ^{1}H NMR spectra of the signals corresponding to the alkylidene proton of the pyrimidinone ring for both UPy polymers. Whereas no concentration-dependent changes are observed for P(nBA)$_n$-C$_6$-UPy **2**, the ^{1}H NMR spectrum of P(nBA)$_n$-C$_2$-UPy **1** shows an additional signal, corresponding to monomeric 2-ureido-6[1*H*]-pyrimidinone at lower concentrations.[33]

To corroborate these findings, concentration-dependent DOSY experiments were performed. As can be observed in Figure 3, the viscosity corrected self-diffusion constant (D_c) of the protons for P(nBA)$_n$-C$_2$-UPy **1** becomes larger upon lowering the concentration. Because the resonances used to calculate the diffusion constant correspond both to the quadruple hydrogen-bonded dimer as well as the monomeric species, the increase in D_c is indicative of an increase in monomeric **1** at lower concentrations.

In sharp contrast, the viscosity corrected self-diffusion constants of the protons of P(nBA)$_n$-C$_6$-UPy **2** are concentration independent between 1 and 0.03 mM [Fig. 3(b)] indicating that solutions of UPy end-functionalized P*n*BA **2** mainly contain quadruple-hydrogen-bonded species in this concentration range [Fig. 3(b)]. The transition from a concentration independent ($c < 0.1$ mM) to a concentration-dependent regime ($c \geq 1$ mM) as is clearly observed for UPy end-functionalized P*n*BA **2** can be attributed to the onset of domain overlap interactions occurring between the polymeric chains. Fitting of the noncorrected self-diffusion constant of P(nBA)$_n$-C$_6$-UPy **2** in the concentration range from 10 mM to 2 mM to a power law ($D_m \sim c^{-\nu}$) gives $\nu = 0.35$ ($R^2 = 0.93$), which deviates somewhat from the theoretical value of $\nu = 0.5$ found by Hess using a theory of phase-space distribution of polymer segments.[34] This discrepancy can be attributed to two effects: First, the width of the crossover regime in which the relation $D_m \sim c^{-0.5}$ holds is small, as was observed experimentally by fluorescence correlation spectroscopy on polystyrene solutions.[35] Second, the theory of

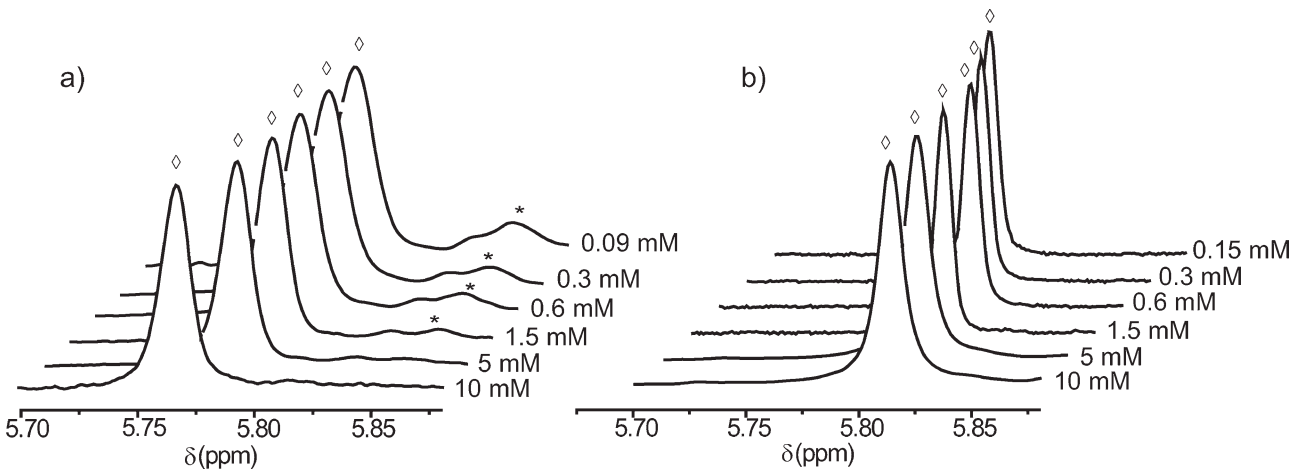

FIGURE 2 Partial ^{1}H NMR spectra (500 MHz) in $CDCl_3$ at 25 °C showing the concentration-dependent changes in the region where the C=CH proton of the 2-ureido-pyrimidinone ring resonates for: (a) P(nBA)$_n$-C$_2$-UPy **1** in which an aliphatic C$_2$ spacer connects the UPy end group with PnBA. (b) P(nBA)$_n$-C$_6$-UPy **2** in which an aliphatic C$_6$ spacer connects the UPy end group with PnBA. The symbols denote signals belonging to dimeric (◇) and monomeric (*) species.

Hess does not take into account the fact that the polymer coils formed by hydrogen-bonded P(*n*BA)$_n$-C$_6$-UPy **2** can exchange with each other because of the reversible nature of the multiple-hydrogen-bonded end groups.

On the basis of the combined concentration-dependent ^{1}H NMR and DOSY study, it can be concluded that the K_{dim} of P(*n*BA)$_n$-C$_6$-UPy **2** is much higher than P(*n*BA)$_n$-C$_2$-UPy **1**. The K_{dim} of P(*n*BA)$_n$-C$_2$-UPy **1** was calculated to be $2 \pm 0.3 \times 10^4$ M^{-1} based on the integral ratio between the signals corresponding to monomeric 2-ureido-6[1*H*]pyrimidinone and dimeric 2-ureido-4[1*H*]pyrimidinone in solutions of **1** at low concentrations. In comparison, the dimerization constant of the UPy dimer substituted with a short aliphatic spacer is 6×10^7 M^{-1} in $CHCl_3$.[36] On the basis of the lowest concentration of the DOSY experiments, the K_{dim} of P(*n*BA)$_n$-C$_6$-UPy **2** is estimated to be $>10^6$ M^{-1}. These results clearly show that the presence of P*n*BA significantly lowers the dimerization constant of the UPy end group, when the aliphatic spacer separating the polymer from the multiple-hydrogen-bonded end group is too short.

The decrease in K_{dim} is presumably caused by favorable, intramolecular hydrogen bonding between the ester groups of P*n*BA, and the hydrogen-bond donors of the UPy group. This backfolding results in a stabilization of the monomeric 6[1*H*] UPy tautomer in agreement with recent results obtained from concentration-dependent studies of EG-substituted 2-ureido-pyrimidinones.[28,29]

Next, the association strength (K_a) of the UPy end-functionalized P*n*BA **1** and **2** with NaPy end-functionalized polymer **3** was probed using UV–Vis titrations. The absorption at $\lambda =$ 355 nm, characteristic for formation of the quadruple hydrogen-bonded UPy·NaPy complex, as a function of added UPy end-functionalized polymer was fitted with a 1:1 binding model governed by an association constant K_a in which one of the components is allowed to self-associate with dimerization constant K_{dim}.[38] Fitting of the absorption at 355 nm as a function of added P(*n*BA)$_n$-C$_2$-UPy **1** (Fig. 4) using the previously determined value of K_{dim} (2×10^4 M^{-1}) resulted in a K_a of $1 \pm 0.4 \times 10^3$ M^{-1} for UPy·NaPy complex **1**·**3**. Given the fact that the K_{dim} of P(*n*BA)$_n$-C$_6$-UPy **2** could not precisely be determined, the absorption data obtained from the titration of **2** and P(*n*BA)$_n$–NaPy **3** was fitted with different values of K_{dim} corresponding to the lowest (10^6 M^{-1}) and highest (6×10^7 M^{-1}) estimate of K_{dim}. In this way, the value of K_a of **2**·**3** was determined to be in the range of 0.4–3×10^6 M^{-1}, which is close to the value of 5×10^6 M^{-1} found for association of UPy and NaPy molecules substituted with apolar, aliphatic substituents.[38,39] The dimerization and association constants of UPy end-functionalized P*n*BA **1** and **2** and NaPy end-functionalized P*n*BA **3** are summarized in Table 2. From these studies, it can be concluded that the heteroassociation constant of UPy end-functionalized P*n*BA polymers with NaPy end-functional PnBA polymers is also significantly lowered when the aliphatic spacer connecting the UPy end group to P*n*BA is too short.

EXPERIMENTAL

Instrumentation

^{1}H NMR and ^{13}C NMR spectra were recorded on a 400 MHz NMR (Varian Mercury, 400 MHz for ^{1}H NMR and 100 MHz for ^{13}C NMR), a 300 MHz NMR (Varian Gemini, 300 MHz for ^{1}H NMR and 75 MHz for ^{13}C NMR) or 500 MHZ NMR (Varian Unity Inova, 500 MHz for ^{1}H NMR and 125 MHz for ^{13}C NMR). Proton chemical shifts are reported in ppm downfield from tetramethylsilane. Matrix-assisted laser desorption/ionization mass-time of flight (MALDI-TOF) spectra were obtained using a PerSeptive Biosystems Voyager-DE PRO spectrometer using an acidic α-cyanohydroxycinnamic acid or a neutral 2-[(2E)-3-(4-*tert*-butylphenyl)-2-methylprop-2-enylidene]malononitrile matrix. Infrared (IR) spectra were recorded on a Perkin Elmer Spectrum One FT-IR spectrometer

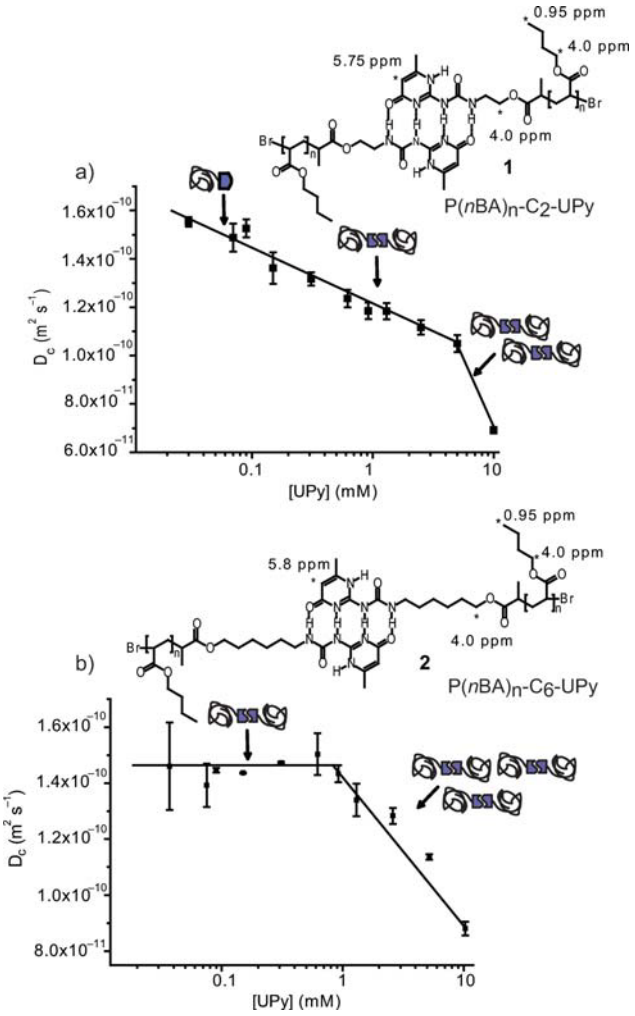

FIGURE 3 Concentration-dependent viscosity corrected diffusion constants (D_c) in $CDCl_3$ at 25 °C for: (a) P(nBA)$_n$-C$_2$-UPy **1** in which an aliphatic C_2 spacer connects the UPy end group with PnBA. (b) P(nBA)$_n$-C$_6$-UPy **2** in which an aliphatic C_6 spacer connects the UPy end group with PnBA. The diffusion constants were acquired using the bipolar pulse pair stimulated echo sequence with convection compensation.[37] The calculated diffusion constant is the average diffusion constant determined for the protons marked with an asterisk. [Color figure can be viewed in the online issue, which is available at wileyonlinelibrary.com.]

with a Universal ATR sampling accessory. Elemental analysis was performed on a Perkin Elmer 2400 series II CHNS/O analyzer. Melting points were determined on a Büchi Melting Point B-540 apparatus.

Materials

All materials were used as received, unless stated otherwise. All reactions were performed under an atmosphere of argon unless noted otherwise. The reactions were followed by thin-layer chromatography (precoated 0.25-mm silica gel plates from Merck), and silica gel column chromatography was carried out with silica gel 60 (mesh 70-230). SEC was carried out at room temperature on a Waters chromatograph connected to a Waters 410 differential refractometer and six Waters Styragel columns (five HR-5 μm and one HWM-20 μm) using THF as eluent (flow rate:1 mL min^{-1}). A Waters 410 differential refractometer and a 996 photodiode array detector were used. The molecular weights of the polymers were calculated relative to linear polystyrene standards. Tetrahydrofuran was dried using a Pure Solv-MD solvent purification system from Advanced Technology. Dichloromethane was distilled over P_2O_5. *n*-Butyl acrylate (*n*BA) was purified by passing over neutral alumina. 2-(1-Imidazolylcarbonylamino)-6-methyl-4-[1*H*]-pyrimidinone was prepared as reported by Keizer.[40]

General Procedures

^{1}H NMR Dilution Experiments and Calculation of K_{dim}

Typical procedure: weighed amounts of UPy end-functionalized polymers **1** and **2** were dissolved in 2.0 mL dry $CDCl_3$ (distilled over P_2O_5) resulting in a 10 mM solution, of which 0.6 mL was injected into the NMR tube. The sample was then diluted to 5.0, 1.5, 0.6, and 0.15 (in the case of P(*n*BA)$_n$-C$_6$-UPy **2**) and 0.09 mM (in the case of P(*n*BA)$_n$-C$_2$-UPy **1**). The peaks in the alkylidene region were deconvoluted using the standard algorithm present in the Varian VNMR software. As the UPy dimer and UPy monomer are in slow exchange on the ^{1}H NMR timescale, it is possible to calculate the molar concentration of monomer and dimer based on the integrals of the NMR signals, the ratio of which is defined as y (I_{mono}/I_{dimer}). From this ratio and the overall UPy concentration U_0, the dimerization constant (K_{dim}) can be calculated using the following equation:[28]

$$K_{dim} = \frac{y(y+1)}{2U_0} \quad (1)$$

Extreme care was taken to keep water levels in the samples as low as possible, because traces of water could lead to the formation of acid in the solution, which interferes with the hydrogen bonding and can lead to degradation of the model compounds. Therefore, all compounds and glassware were dried over P_2O_5 and $CDCl_3$ was distilled over P_2O_5 and stored over molecular sieves. With this procedure, water levels in the samples were below the detection limit of standard Karl-Fischer titrations. The ^{1}H NMR dilution experiments were performed on a Varian Unity Inova 500 MHz NMR equipped with a 5-mm ^{1}H/X Inverse Detection probe with gradient capabilities.

UV–Vis Titrations

UV/Vis spectra were recorded using 1-cm path length cells on a Perkin Elmer Lambda 40P equipped with a PTP-1 Peltier temperature control system. At 25 °C, a series of spectra were obtained by the addition of μL amounts of a stock solution containing 25.3 μM of the NaPy end-functionalized P*n*BA polymer (**3**) and 300 μM of the UPy end-functionalized P*n*BA polymer (either **1** or **2**) in $CHCl_3$ to a cell containing 2.0 mL of a 25.3 μM solution of the NaPy end-functionalized polymer (**3**). All obtained traces were base-line corrected. The association constant (K_a) was determined using a previously established protocol as outlined in ref. [38]. Because the PDIs of the two UPy polymers are similar, errors that are introduced by the uncertainty in the concentration of end

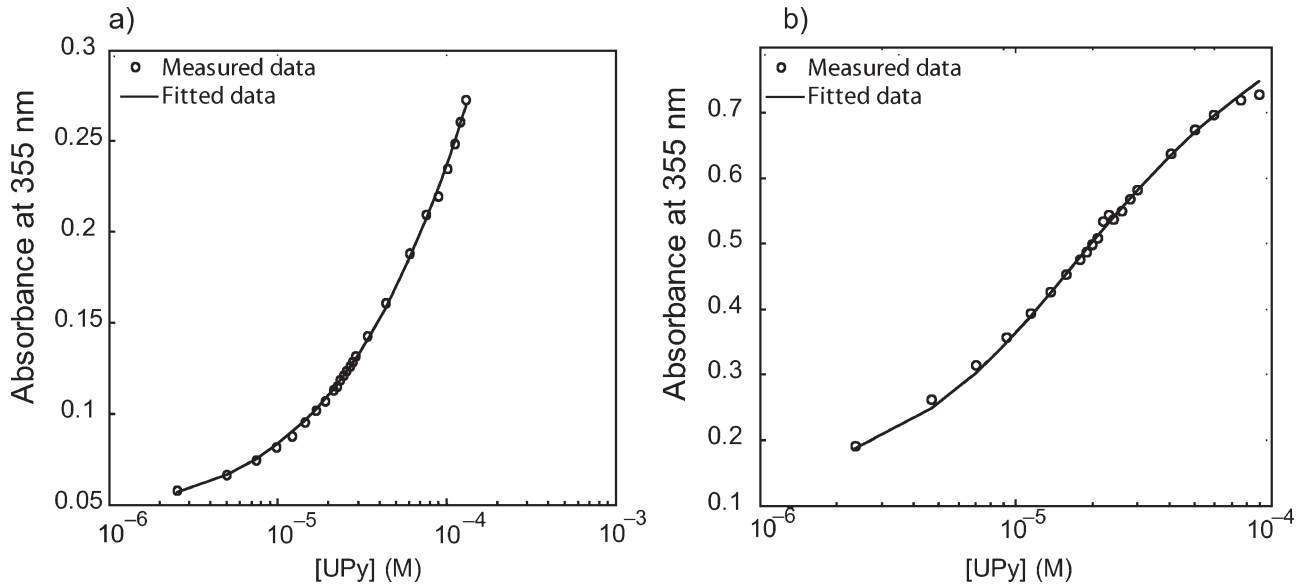

FIGURE 4 (a) Plot of absorbance at 355 nm for a solution containing 2.53×10^{-5} M of P(nBA)$_n$-NaPy **3** upon consecutive additions of aliquots of P(nBA)$_n$-C_2-UPy **1** in $CHCl_3$ at 25 °C. The solid line represents the best fit of the data ($K_a = 1.2 \pm 0.4 \times 10^3$ M^{-1}) to the 1:1 binding model with one dimerizing component ($K_{dim} = 1.7 \times 10^4$ M^{-1}). (b) Plot of absorbance at 355 nm for a solution containing 2.53×10^{-5} M of P(nBA)$_n$-NaPy **3** upon consecutive additions of aliquots of P(nBA)$_n$-C_6-UPy **2** in $CHCl_3$ at 25 °C. The solid line represents the best fit of the data ($K_a = 3 \pm 0.6 \times 10^6$ M^{-1}) to the 1:1 binding model with one dimerizing component ($K_{dim} = 6 \times 10^7$ M^{-1}).

groups are approximately equal, and hence, a quantitative comparison of K_a between the two polymers is justified.

Diffusion-Ordered Spectroscopy

Concentration-dependent DOSY experiments on end-functionalized UPy polymers **1** and **2** in $CDCl_3$ were performed on a Varian Unity Inova 500 MHz NMR equipped with a 5-mm ^1H/X Inverse Detection probe with gradient capabilities (Performa II/III, maximum gradient strength of 70 G cm^{-1}) at 25 °C. Dry $CDCl_3$ used for the dilution studies was obtained by adding oven dried molecular sieves (4 Å) 48 h before the measurements. The $CDCl_3$ used for the concentration-dependent DOSY studies on end-functionalized UPy polymers **2** and **3** was distilled over P_2O_5 before use. The NMR tubes (5 mm) used for the studies were dried over P_2O_5 under high vacuum. Samples were not spinning during the measurements. A 5-min temperature calibration period was provided before analysis. The DOSY bipolar pulse pair stimulated echo with convection compensation (Dbppste_cc) sequence[37] was used for the determination of the self-diffusion of the different components. Temperature calibration was achieved by observing the temperature-dependent chemical-shift separation between the OH and CH_3 resonance in methanol. In all experiments, the 90° pulse widths were determined. The strength of the B_0 field gradient was calibrated by measuring the self-diffusion coefficient of the residual HDO signal in a 1% D_2O sample, at 25 °C ($D(H_2O) = 19 \times 10^{-10}$ m^2 s^{-1}).[41] The experimental diffusion constant (D_m) was obtained using the Stejskal–Tanner[42] equation:

$$I(G_{zi}) = I(0)\exp(-D_m\gamma_h^2\delta^2(G_{zi})^2(\Delta - \delta/3 - \tau/2)) \qquad (2)$$

$I(G_{zi})$ represents the experimental signal intensity at a gradient-level of G_{zi} (G cm^{-1}), $I(0)$ is the initial signal intensity, γ_h is the magnetogyric ratio for ^1H, τ is the time interval between the bipolar pulse pair, δ is the length of the pulsed field gradient, and Δ is the diffusion period. Using this equation, it is possible to determine D_m from a plot of $\ln(I(G_{zi})/I(0))$ versus G_{zi}^2. In a typical experiment, 32 transients (with a recycle delay of 3 s per transient) for each of the 100 steps were recorded with increasing gradient strength (ranging from an initial value of 1.085–32.55 G cm^{-1}), and gradient pulse duration, diffusion delay, and maximum gradient strength were adjusted at each concentration to obtain an 80% reduction of the signal at the highest gradient strength. At each concentration the 90° ^1H pulse width was calibrated at a transmitter power of 58 dB.

The viscosity corrected diffusion constant (D_c) was calculated using the following equation:

$$D_c = D_m \times \frac{D_{sol,pure}}{D_{sol,m}} \qquad (3)$$

D_m and $D_{sol,m}$ represent the measured values for the solute and the residual solvent peak ($CHCl_3$), respectively, and $D_{sol,}$

TABLE 2 UPy Dimerization Constant (K_{dim}) and UPy·NaPy Association Constant (K_a) of UPy End-Functionalized P*n*BA **1** and **2** and NaPy End-Functionalized P*n*BA **3** in $CDCl_3$ (K_{dim}) and $CHCl_3$ (K_a) at 25 °C

Polymer	Spacer Length	K_{dim} (M^{-1})	K_a (M^{-1})
1	C_2	$2 \pm 0.3 \times 10^4$	$1 \pm 0.4 \times 10^3$
2	C_6	$>10^6$	$0.4–3 \times 10^6$

$_{pure}$ is the diffusion constant measured for the residual $CHCl_3$ in pure $CDCl_3$.

Synthesis

Synthesis of 6-(tert-Butoxycarbonylamino)hexyl 2-bromopropanoate (4)

Boc protected 6-aminohexanol (4.4 g, 20 mmol) was dissolved in 40 mL of dichloromethane, and 1.87 mL (24 mmol, 1.92 g) pyridine was added, and the solution was cooled to 0 °C. After this, 2-bromopropionyl bromide (4.75 g, 22 mmol) was added dropwise via a syringe. The solution was stirred for 12 h, and it was allowed to warm to room temperature (careful: do not to let the temperature become higher). The solution was transferred to a separatory funnel and washed with 1 M HCl (3× 500 mL), saturated $NaHCO_3$ (3× 500 mL) and brine (1× 100 mL), after which the organic layer was dried with $MgSO_4$ and evaporated *in vacuo*. Column chromatography (SiO_2, $CHCl_3$ as an eluent) afforded 4.5 g of **4** as a colorless oil. Yield: 64%. ^{1}H NMR ($CDCl_3$): δ = 4.54 (b, 1H, N*H*), 4.34 (q, 1H, C*H*—Br), 4.16 (m, 2H, O—CH_2), 3.08 (m, 2H, CH_2—NH), 1.81 (d, 3H, CH—CH_3), 1.68–1.31 (m, 17H, CH_2 and CH_3). ^{13}C NMR ($CDCl_3$): δ = 170.2, 156.0, 79.0, 65.8, 40.4, 40.2, 29.9, 28.6, 28.4, 28.3, 27.8, 26.3, 25.4, 21.6. IR (ATR): ν = 3349, 2976, 2933, 2862, 1737, 1697, 1517, 1448, 1391, 1366, 1337, 1269, 1249, 1227, 1163, 1071, 991 cm^{-1}. MALDI-TOF-MS (m/z): calcd: 351.10. Observed: 374.14 (MNa^+). Anal. Calcd for $C_{14}H_{26}BrNO_4$: C 47.73, H 7.44, N 3.98; Found: 48.10, H 7.31, N 3.85.

Synthesis of 6-Aminohexyl 2-bromopropanoate (Obtained as TFA Salt) (5)

A solution of 6-(*tert*-butoxycarbonylamino)hexyl 2-bromopropanoate (0.60 g, 1.7 mmol) in freshly distilled dichloromethane was cooled to 0 °C. Subsequently, 5 mL (1.48 g, 12.9 mmol of trifluoroacetic acid) of a 20 % (v/v) solution of trifluoroacetic acid (anhydrous)/dichloromethane (freshly distilled) was added dropwise via a syringe. The solution was allowed to warm to room temperature and stirred for an additional 12 h. Evaporation *in vacuo* and extensive drying resulted in 0.58 g of **5** as colorless oil. Yield: 93%. ^{1}H NMR ($CDCl_3$): δ = 7.73 (b, 3H, NH_3^+), 4.36 (q, 1H, C*H*—Br), 4.16 (m, 2H, O—CH_2), 2.96 (b, 2H, CH_2—NH_3^+), 1.81 (d, 3H, CH—CH_3), 1.68–1.41 (m, 8H, CH_2). ^{13}C NMR ($CDCl_3$): δ = 170.6, 65.5, 40.2, 39.9, 27.9, 27.2, 25.6, 24.9, 21.5. IR (ATR): ν = 3450, 2940, 2866, 1779, 1734, 1672, 1529, 1469, 1447, 1431, 1392, 1381, 1337, 1276, 1199, 1133, 1063, 990.9 cm^{-1}. MALDI-TOF-MS (m/z): calcd: 252.06. Observed: 252.11.

Synthesis of 6-(3-(6-Methyl-4-oxo-1,4-dihydropyrimidin-2-yl)ureido)hexyl-bromopropanoate (6)

To a solution of 2-(1-imidazolylcarbonylamino)-6-methyl-4-[1*H*]-pyrimidinone (0.39 g, 1.90 mmol) and TFA salt **5** (0.58 g, 1.6 mmol) in 10 mL $CHCl_3$ was added 1 mL of triethylamine (0.72 g, 7.2 mmol). Subsequently, the solution was stirred for 12 h at a temperature of 45 °C after which the solution was cooled and 20 mL of $CHCl_3$ was added. The organic phase was washed with aqueous 1 M HCl (4× 100 mL), saturated $NaHCO_3$ (2× 70 mL) and brine (1× 100 mL) and dried with $MgSO_4$. Evaporation *in vacuo* and column chromatography (1% MeOH/$CHCl_3$ as an eluent) resulted in pure **6** as an off white solid, mp: 159 °C. Yield: 50%. ^{1}H NMR ($CDCl_3$): δ = 13.11 (b, 1H, NH), 11.86 (b, 1H, NH), 10.17 (b, 1H, NH), 5.82 (s, 1H, CH_1), 4.35 (q, 1H, C*H*—Br), 4.17 (m, 2H, O—CH_2), 3.25 (m, 2H, CH_2—NH), 2.23 (s, 3H, CH_3), 1.81 (d, 3H, CH—CH_3), 1.69–1.39 (m, 8H, CH_2). ^{13}C NMR ($CDCl_3$): δ = 173.0, 170.3, 156.6, 154.7, 148.2, 106.7, 66.0, 40.2, 39.8, 29.4, 28.3, 26.5, 25.5, 21.7, 18.9. IR (ATR): ν = 2937, 2856, 1735, 1698, 1666, 1582, 1525, 1445, 1338, 1307, 1257, 1227, 1163, 1138, 942 cm^{-1}. MALDI-TOF-MS (m/z): calcd: 402.09. Observed: 404.03 (MH^+), 425.02 (MNa^+). Anal. Calcd for $C_{15}H_{23}BrN_4O_4$: C 44.68, H 5.75, N 13.89; Found: 44.77, H 5.55, N 14.05.

Synthesis of UPy End-Functional Poly(n-butyl acrylate), P(nBA)$_n$-C$_6$-UPy (2)

n-Butyl acrylate (*n*BA, 3.00 g, 23.4 mmol), UPy initiator **6** (34.7 mg, 0.23 mmol), PMDETA (81 mg, 0.47 mmol) were combined in a Schlenk flask and subjected to three freeze–pump–thaw cycles. CuBr (12 mg, 0.24 mmol) was added under flowing nitrogen, and the flask was evacuated and backfilled with nitrogen twice. The flask was then sealed and placed in a 70 °C oil bath for 3 h before exposing to air and diluting with THF. The reaction mixture was passed over neutral alumina to remove the copper, concentrated, and precipitated into cold hexanes to give P(*n*BA)$_n$-C$_6$-UPy **2**. After drying, the resulting oil was dissolved in 50 mL of $CHCl_3$ and washed with an aqueous solution of 0.01 M EDTA (3× 100 mL), saturated $NaHCO_3$ (2× 50 mL), and brine (1× 100 mL). Evaporation of the organic layer *in vacuo* resulted in a sticky oil which was dried over P_2O_5 *in vacuo* at a temperature of 50 °C. M_n = 8.9 kDa, PDI = 1.1 (SEC, THF). ^{1}H NMR ($CHCl_3$): δ = 13.11, 11.85, 10.17, 5.81, 4.2–3.9, 3.2, 2.4–2.2, 1.90–0.79.

CONCLUSIONS

Two UPy end-functionalized P*n*BA polymers, P(*n*BA)$_n$-C$_2$-UPy **1** and P(*n*BA)$_n$-C$_2$-UPy **2**, were prepared using ATRP from UPy-functional initiators. Given the similar molecular weights of the polymers, these end-functionalized polymers primarily differ in the length of the aliphatic spacer separating the P*n*BA from the UPy group. Concentration-dependent ^{1}H NMR and DOSY experiments clearly show that the dimerization constant of the UPy end-functionalized P*n*BA polymer, where a short C$_2$ spacer separates the UPy group from the P*n*BA is lowered as a result of competitive intramolecular noncovalent interactions. In addition, the heteroassociation strength of this polymer with a NaPy end-functionalized P*n*BA is drastically lowered. In contrast, when a longer C$_6$ aliphatic spacer separates the UPy end group from the P*n*BA polymer, the dimerization and heteroassociation strengths are largely unaffected. These results clearly show the necessity for the incorporation of a large aliphatic spacer in the design of supramolecular diblock copolymers when polar polymers such as P*n*BA are used. Although not the focus of this study, we expect that the decrease in association constant as a result of competitive intramolecular interactions will have a

profound effect on the thermomechanical properties of UPy-based materials.

The authors acknowledge Mr. J. van Dongen, Dr. X. Lou, Mr. Ralf Bovee, and Mr. H. Eding for technical assistance. This work is supported by the Council for Chemical Sciences of The Netherlands Organization for Scientific Research (CW-NWO). This work was also supported by the National Science Foundation (MRSEC Program DMR-05204156 (MRL-UCSB)) and made use of the Materials Research Laboratory Central Facilities, supported by the MRSEC Program of the NSF under Award No. DMR05-20415; a member of the NSF-funded Materials Research Facilities Network www.mrfn.org.

REFERENCES AND NOTES

1 Tang, C.; Lennon, E. M.; Fredrickson, G. H.; Kramer, E. J.; Hawker, C. J. Science 2008, 322, 429–432.

2 Xu, T.; Zhao, N.; Ren, F.; Hourani, R.; Lee, M. T.; Shu, J. Y.; Mao, S.; Helms, B. A. ACS Nano 2011, 5, 1376–1384.

3 Suchao-In, N.; De Bruyn, H.; Perrier, S.; Chirachanchai, S. J. Polym. Sci. Part A: Polym. Chem. 2009, 47, 6783–6788.

4 Lin, H.-C.; Jiang, M.-D.; Wu, S.-C.; Jou, L.-K.; Chou, K.-P.; Huang, C.-M.; Wei, K.-H J. Polym. Sci., Part A: Polym. Chem. 2009, 47, 4685–4702.

5 Feng, E. H.; Lee, W. B.; Fredrickson, G. H. Macromolecules 2007, 40, 693–702.

6 Tanaka, F.; Ishida, M.; Matsuyama, A. Macromolecules 1991, 24, 5582–5589.

7 Han, Y.; Jiang, W. J. Phys. Chem. B 2011, 115, 2167–2172.

8 Huh, J.; ten Brinke, G. J. Chem. Phys. 1998, 109, 789–797.

9 Angerman, H. J.; ten Brinke, G. Macromolecules 1999, 32, 6813–6820.

10 Anthamatten, M J. Polym. Sci. Part B: Polym. Phys. 2007, 45, 3285–3299.

11 Yang, X.; Hua, F.; Yamato, K.; Ruckenstein, E.; Gong, B.; Kim, W.; Ryu, C. Y. Angew. Chem., Int. Ed. 2004, 43, 6471–6474.

12 Feldman, K. E.; Kade, M. J.; de Greef, T. F. A.; Meijer, E. W.; Kramer, E. J.; Hawker, C. J. Macromolecules 2008, 41, 4694–4700.

13 Feldman, K. E.; Kade, M. J.; Meijer, E. W.; Hawker, C. J.; Kramer, E. J. Macromolecules 2010, 43, 5121–5127.

14 Noro, A.; Nagata, Y.; Takano, A.; Matsushita, Y. Biomacromolecules 2006, 7, 1696–1699.

15 Wrue, M. H.; McUmber, A. C.; Anthamatten, M. Macromolecules 2009, 42, 9255–9262.

16 Binder, W. H.; Bernstoff, S.; Kluger, C.; Petraru, L.; Kunz, M. J. Adv. Mater. 2005, 17, 2824–2828.

17 Ambade, A. V.; Burd, C.; Higley, M. N.; Nair, K. P.; Weck, M. Chem.-Eur. J. 2009, 15, 11904–11911.

18 Mather, B. D.; Lizotte, J. R.; Long, T. E. Macromolecules 2004, 37, 9331–9337.

19 Vora, A.; Zhao, B.; To, D.; Cheng, J. Y.; Nelson, A. Macromolecules 2010, 43, 1199–1202.

20 Celiz, A. D.; Scherman, O. A. J. Polym. Sci. Part A: Polym. Chem. 2010, 24, 5833–5841.

21 Huh, J.; Jung, J. Y.; Lee, J. U.; Cho, H.; Park, S.; Park, C.; Jo, W. H. ACS Nano 2011, 5, 115–122.

22 Lohmeijer, B. G. G.; Schubert, U. S. Angew. Chem., Int. Ed. 2002, 41, 3825–3829.

23 Moughton, A. O.; O'Reilly, R. K. J. Am. Chem. Soc. 2008, 130, 8714–8725.

24 Rauwald, U.; Scherman, O. A. Angew. Chem. Int. Ed. 2008, 47, 1–5.

25 Yan, Q.; Yuan, J.; Cai, Z.; Xin, Y.; Kang, Y.; Yin, Y. J. Am. Chem. Soc. 2010, 132, 9268–9270.

26 Lee, M.; Schoonover, D. V.; Gies, A. P.; Hercules, D. M.; Gibson, H. W. Macromolecules 2009, 42, 6483–6494.

27 Shen, J.; Hogen-Esch, T. J. Am. Chem. Soc. 2008, 130, 10866–108667.

28 de Greef, T. F. A.; Nieuwenhuizen, M. M. L.; Stals, P. J. M.; Fitié, C. F. C.; Palmans, A. R. A.; Sijbesma, R. P.; Meijer, E. W Chem. Commun. 2008,4306–4308.

29 de Greef, T. F. A.; Nieuwenhuizen, M. M. L.; Sijbesma, R. P.; Meijer, E. W. J. Org. Chem. 2010, 75, 598–610.

30 Park, T.; Todd, E. M.; Nakashima, S.; Zimmerman, S. C. J. Am. Chem. Soc. 2005, 127, 18133-18142.

31 Wang, X.-Z.; Li, X.-Q.; Shao, X.-B.; Zhao, X.; Deng, P.; Jiang, X.-K.; Li, Z.-T.; Chen, Y.-Q. Chem. Eur. J. 2003, 9, 2904–2913.

32 Huang, J. Y.; Pintauer, T.; Matyjaszewski, K. J. Polym. Sci. Part A: Polym. Chem. 2004, 42, 3285–3292.

33 We have previously shown[29] that the extinction coefficient at $\lambda = 285$ nm can be related to the concentration of monomeric UPy in the 6[1*H*] tautomeric form. Indeed, UV–Vis spectra of UPy end-functionalized UPy P*n*BA polymers **1** and **2** in $CHCl_3$ at a concentration of 0.05 mM clearly show that the extinction coefficient of P(nBA)$_n$-C_2-UPy **1** at 285 nm is much higher than the extinction coefficient of P(nBA)$_n$-C_6-UPy **2** at the same wavelength, indicating an increased fraction of the monomeric 6[1*H*] UPy tautomer in the first.

34 (a) Hess, W. Macromolecules 1986, 19, 1395–1404; (b) Hess, W. Macromolecules 1987, 20, 2587–2599.

35 Liu, R.; Gao, X.; Adams, J.; Opperman, W. Macromolecules 2005, 38, 8845–8849.

36 Sontjens, S. H. M.; Sijbesma, R. P.; van Genderen, M. H. P.; Meijer, E. W. J. Am. Chem. Soc. 2000, 122, 7487–7493.

37 Jerschow, A.; Muller, N. J. Magn. Reson. 1997, 125, 372–375.

38 de Greef, T. F. A.; Ligthart, G. B. W. L.; Lutz, M.; Spek, A. L.; Meijer, E. W.; Sijbesma, R. P. J. Am. Chem. Soc. 2008, 130, 5479–5486.

39 Ligthart, G. B. W. L.; Ohkawa, H.; Sijbesma, R. P.; Meijer, E. W. J. Am. Chem. Soc. 2005, 127, 810–811.

40 Keizer, H. M.; Sijbesma, R. P.; Meijer, E. W. Eur. J. Org. Chem. 2004, 12, 2553–2555.

41 Longsworth, L. G. J. Phys. Chem. 1960, 64, 1914–1917.

42 Stejskal, E. O.; Tanner, J. E. J. Chem. Phys. 1965, 42, 288–292.